On-Chip Decoupling Zone For Package-Stress Reduction

V.L. Spiering, S. Bouwstra, R.M.E.J. Spiering*, M. Elwenspoek

MESA, Institute for Micro Electronics, Materials Engineering, Sensors & Actuators
** Faculty of Mechanical Engineering*
University of Twente, P.O. Box 217, 7500 AE Enschede, The Netherlands

Abstract

This paper reports the reduction of package-stresses by introducing a decoupling zone directly around a sensor structure. Different geometries of the decoupling zones are compared, using the Finite Element Method (FEM) and analytical models. A large reduction is obtained in case of a corrugated decoupling zone. To optimize the reduction, an analytical description of a ring-shaped V-groove is given. Finally the influence of a backplate mounted to the sensor chip is discussed.

Introduction

Micromechanical sensors show a high sensitivity to mechanical stresses. Unwanted stresses like encapsulation-stresses and thermally induced stresses during operation can jam the sensor-output. Several proposals to reduce these stresses have been reported on [1]-[3]. A large reduction of unwanted stresses is obtained by introducing a decoupling zone directly around the sensor structure, see figure 1. Compared with a decoupling zone in an intermediate-chip [1] the advantages of this concept are (1) an aditional intermediate is avoided, (2) there is no bonding-interface within the decoupling zone and (3) the reduction caused by the tangential stiffness of the circular zone is very large. With the use of analytical expressions, verified by FEM-calculations, it is possible to optimize the geometry of the decoupling zone and backplate.

Fig. 1 A sensor-diaphragm surrounded by a corrugated decoupling zone.

In this paper the reduction of thermally induced stresses in a silicon diaphragm surrounded by a flat or corrugated zone will be presented. The whole structure consists of a silicon chip with a diaphragm (the sensing part) and a decoupling zone, mounted on a steel backplate. Figure 2 shows the different options for the decoupling zone. The thermal mismatch of the chip and the backplate causes stresses which fluctuate with the ambient temperature.

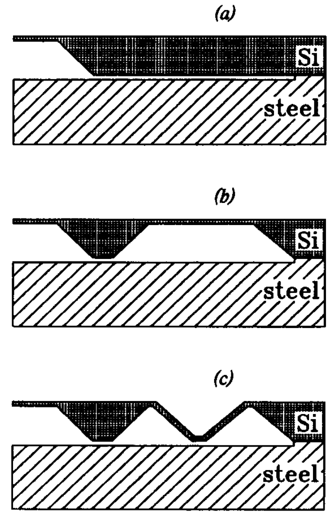

Fig. 2 Cross-section of the considered axisymmetric structures with three different options for the decoupling zone: (a) without zone, (b) flat zone and (c) the corrugated zone.

When the structures of figure 2 are loaded by a uniform temperature there will be two results of interest (see figure 3): the planar stress σ and the centre-deflection v_1 of the deformed diaphragm, where v_1 is a measure for bending. To analyze the influence of the backplate and the decoupling zone on σ and v_1, both parts will be investigated seperately.

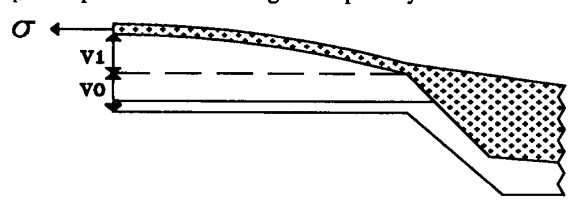

Fig. 3 Planar stress σ and deflections v_0 and v_1 of the diaphragm, due to deformation of the complete structure.

Results

Comparison of the zones

Figure 4 shows an example of the reduction of the planar stress in the diaphragm when a radial displacement U is imposed on the outer edge of the silicon chip. The diaphragm used for this calculations has a radius of 0.5 mm and thickness 2 μm. The zones have the same thickness as the diaphragm and inner c.q. outer radii of 1.5 and 2.25 mm. The corrugated zone here consists of one V-corrugation over the entire depth of the chip (380 μm). The description of the analytical calculations is given in the appendix.

91CH2817-5/91/0000-0982$01.00

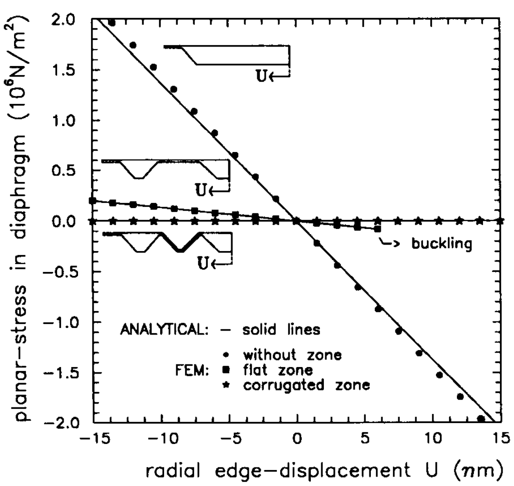

Fig. 4 Analytical and FEM-results for planar stress in the diaphragm as a function of the imposed radial displacement U at the edge.

The reduction of the planar stress using a flat or corrugated zone is clearly visible. For a certain displacement U buckling occurs in the flat decoupling zone; the slope of the curve beyond the buckling point, which was not included in these models, nearly equals half the slope before buckling. The reduction of the planar stress in case of the corrugated zone compared to no-zone can easily reach factors higher than 1000.

The V-corrugation

Parameters to optimize the reduction of one V-corrugation are the depth H, the thickness t, the inner radius r_{in} and the angle γ (see figure 5). In the calculations γ was always 54.74 degrees.

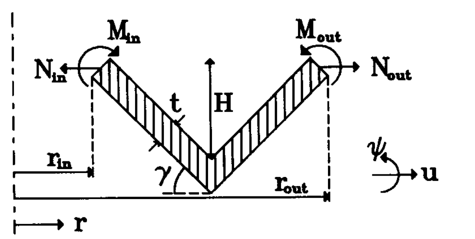

Fig. 5 Definition of the parameters of the axisymmetrical V-corrugation.

In order to evaluate the V-corrugation the inner radius is clamped for radial displacements u and rotations ψ, but free to move in axial direction. In that case no axial forces occur in the corrugation. At the outer radius there will be either an imposed displacement $u=u_{out}$ or an imposed rotation $\psi=\psi_{out}$, remaining degrees of freedom are suppressed. Figure 6 shows the displacement u and the radial planar force as a function of the radius in a V-corrugation under an imposed displacement of the outer radius. The analytical results are based on the theory of conical shells (see appendix). They were checked by FEM-calculations with axisymmetrical shell-elements and differences were smaller than 1 %. Note that by using these elements it is difficult to find good FEM-results for the planar force at points close to the symmetry-axis because of problems with convergence. The discontinuity in the derivative of the radial displacement at the bottom of the V-corrugation was also observed in the FEM-results.

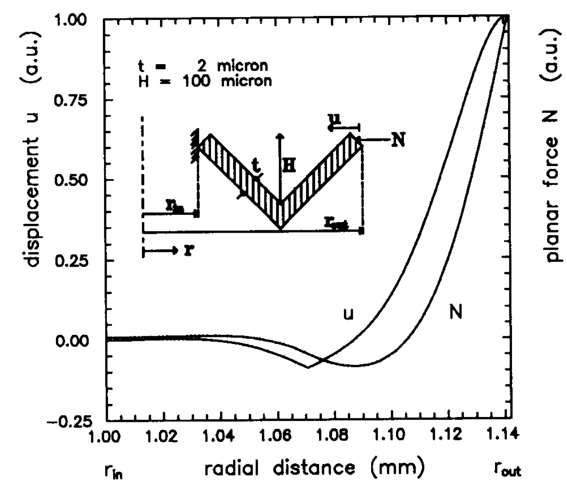

Fig. 6 The displacement u and the planar force N as a function of the radial distance in a silicon V-corrugation: H=100 µm, t=2 µm and γ=54.74 degrees.

To quantify the reduction two reduction factors are defined: the planar force reduction N_{out}/N_{in} and the moment reduction M_{out}/M_{in}, and both have a value at an imposed displacement and an imposed rotation. Figures 7 and 8 show the reduction factors for the planar force as a function of the depth H and thickness t of the corrugation parameterized for the inner radius r_{in}. The load was an imposed displacement but an imposed rotation gives similar results. Also the moment reduction which gives similar results for both load cases is not shown here.

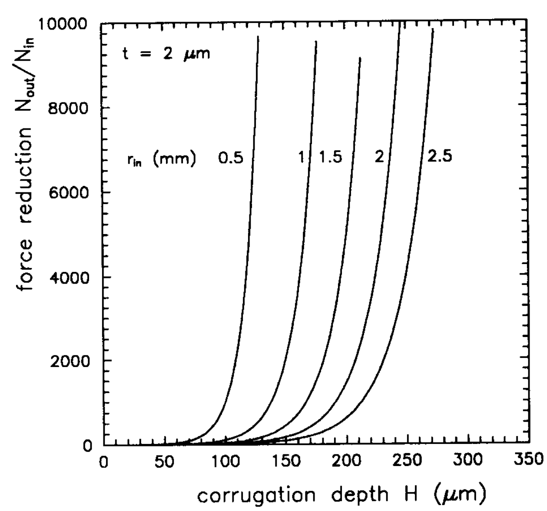

Fig. 7 Analytical results for the planar force reduction as a function of the corrugation depth H for a V-corrugation with thickness t=2 µm and inner radius r_{in} as parameter.

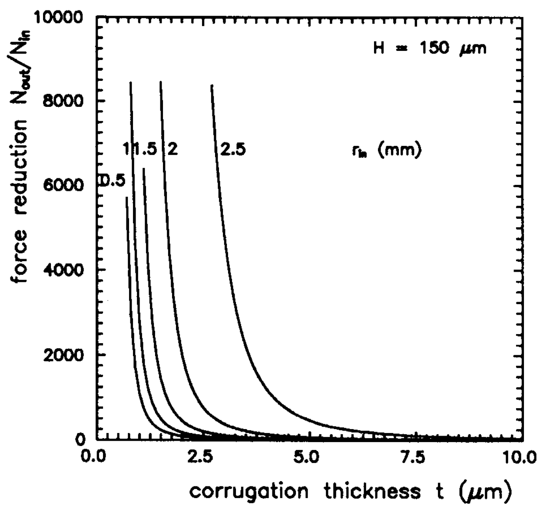

Fig. 8 Analytical results for the planar force reduction as a function of the thickness t for a V-corrugation with depth H=150 μm and inner radius r_{in} as parameter.

According to equation (11) of the appendix there is the rule of thumb:

$$\boxed{\text{reduction } N_{out}/N_{in} \text{ or } M_{out}/M_{in} = f_{red}\cdot e^{K}} \quad (1)$$

$$\text{with} \quad K = \sqrt{\frac{4\sqrt{3(1-\nu^2)}}{t\cos\gamma}}\cdot\left(\sqrt{2H+r_{in}\tan\gamma}-\sqrt{r_{in}\tan\gamma}\right) \quad (2)$$

where f_{red} is constant in a certain range and ν is the poisson's ratio. For dimensions within the range $0.25 < H^2/(t \cdot r_{in}) < 40$ is found that:

$$f_{red} = 5 \pm 1$$

This design-rule is very useful for estimating a reduction without making the calculations described in the appendix. Outside the range care should be taken by applying the design-rule. Also the calculations have their limits of application because the shell-theory is based on small values of t/H.

The backplate

The influence of the thickness of a backplate, mounted to the sensor chip (without decoupling zone) will be discussed briefly. For the analytical calculations the diaphragm, chip and backplate were considered as plates, see also the appendix. At the interfaces between diaphragm and chip as well as chip and backplate the rotations are assumed to be equal. This means that deformations are due to bending and planar elongation only and local effects at the interfaces are ignored. Figure 9 shows the results for the planar stress σ in the diaphragm and the displacement v_1 (bending, see also figure 2), due to the thermal mismatch between chip and backplate, as a function of the thickness of the backplate.

The sign of the stress in the diaphragm depends on the thickness of the backplate, i.e. there is an optimal backplate thickness, resulting in a zero diaphragm stress. At this thickness of the backplate bending and radial elongation of the complete structure compensate each other with respect to their influence on the planar stress in the diaphragm.

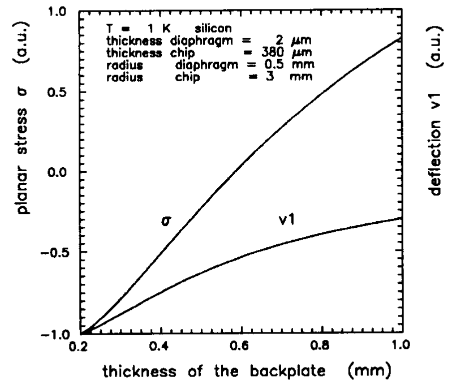

Fig. 9 Analytical results for the planar stress σ and the deflection v_1, due to the thermal mismatch between sensor chip and backplate, as a function of the thickness of the backplate.

Conclusions

It is shown that it is possible to reduce (package) stresses by introducing a decoupling zone around a sensor structure. Reduction factors over 1000 and higher can be realized by using an axisymmetrical V-corrugation. A design rule to optimize the reduction for the V-corrugation is given. This rule is based on analytical calculations and verified by FEM-simulations. Finally it is shown that the thickness of a back-plate, mounted to the sensor chip, can be optimized for minimal thermal stresses in the sensor.

Acknowledgement

The authors would like to thank dr. Bert Geijselaars for helpful discussions and suggestions.

References

[1] H.L. Offereins, H. Sandmaier, "Novel Stress Free Assembly Technique for Micromechanical devices", *Proc. Micro System Technologies 90, Berlin, Germany, Sept. 10-13 1990*, pp. 515-520.

[2] B. Hälg, R.S. Popovic, "How to liberate Integrated Sensors from Encapsulation Stress", *Sensors & Actuators A21-A23 (1990)*, 908-910.

[3] W. Germer, G. Kowalski, "Mechanical Decoupling of Monolithic Pressure Sensors in Small Plastic Encapsulations", *Sensors and Actuators A21-A23 (1990)*, 1065-1069.

[4] S.P. Timoshenko and J.N. Goodier, "Theory of elasticity", McGraw-Hill, 3rd ed., 1982, pp. 65-80.

[5] S. Timoshenko and S. Woinowski-Krieger, "Theory of plates and shells", McGraw-Hill, 2nd ed., 1970, pp. 51-63.

[6] F.I. Niordson, "Shell theory", North-Holland, 1985, pp. 272-281.

[7] M. Abramowitz and I.A. Stegun, "Handbook of mathematical functions", section 9.9 and 9.10, Dover Publications, New York.

Appendix

The whole structure will be divided into 5 parts:
1: The diaphragm
2: Inner ring of the chip
3: The decoupling zone
4: Outer ring of the chip
5: The backplate

If the relations between the displacements, rotations, planar forces and moments are known for each part, then connection of the parts, applying the equilibrium of forces and of moments as well as the continuity of displacements and of rotations at the interfaces, yields the total solution.

a. Diaphragm, chip, flat zone and backplate.

The flat zone, diaphragm and all thick parts of the chip will be considered as plates with a bending moment and a radial planar force at the edges, see figure 10.

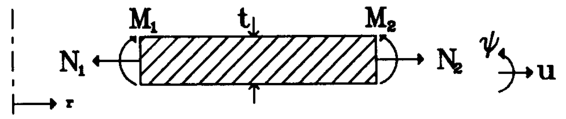

Fig. 10 Definition of the plate for the description of the diaphragm, of the flat zone, of inner and outer ring of the chip and of the backplate.

Expressions for the radial displacements u(r) and the rotations ψ(r) as a function of the planar force per unit width N_i and the bending moments M_i, are known from elementary mechanics ([4],[5]). Equilibrium of forces and moments together with continuity of displacements and rotations at the edges gives all the equations necessary for the solution. A thermal load will be realised in this case by creating an initial strain $\varepsilon=\Delta\alpha\cdot\Delta T$ where $\Delta\alpha$ is the difference in the thermal expansion coefficients of the backplate and silicon. ΔT is the difference between the ambient temperature and a reference temperature (e.g. room temperature). Note that in the case of connecting two plates with different thicknesses and nonsymmetry in the axial direction there are two additional contributions at the interfaces: 1) at the equilibrium of moments the planar force of the connecting plate gives a contribution and 2) at the continuity of displacements the rotation of the connecting plate gives a contribution.

b. Conical shell and V-corrugation

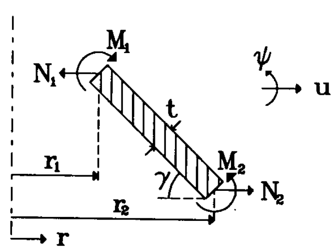

Fig. 11 Definition of the conical shell for the description of the V-corrugation.

In the description of the conical shell the axial force will be kept zero. This is the case if one of the edges is free to move in the axial direction. The solution for a conical shell with an angle γ as in figure 11 and with a thickness t is then found to be [6]:

$$u = \frac{D\rho^2\cos^2\gamma}{Et\sin\gamma}\,[A_1(2\nu\,bei_2x - x\,bei_2'x) - A_2(2\nu\,ber_2x - x\,ber_2'x) + B_1(2\nu\,kei_2x - x\,kei_2'x) - B_2(2\nu\,ker_2x - x\,ker_2'x)] \quad (3)$$

$$N = \frac{-16D\rho^4}{x^2\sin\gamma}\,[A_1 bei_2x - A_2 ber_2x + B_1 kei_2x - B_2 ker_2x] \quad (4)$$

$$\psi = A_1 ber_2x + A_2 bei_2x + B_1 ker_2x + B_2 kei_2x \quad (5)$$

$$M = \frac{4D\rho^2}{x^2}\,[A_1(2\nu x\,ber_2'x + ber_2x) + A_2(2\nu x\,bei_2'x + bei_2x) + B_1(2\nu x\,ker_2'x + ker_2x) + B_2(2\nu x\,kei_2'x + kei_2x)] \quad (6)$$

where $$\rho^2 = \frac{\sqrt{3(1-\nu^2)}}{t}\tan\gamma \quad , \quad D = \frac{Et^3}{12(1-\nu^2)} \quad (7)$$

and $$x = 2\rho\sqrt{\frac{2r}{\cos\gamma}} \quad (8)$$

E is the modulus of elasticity and ν the Poisson's ratio. Ber_2, bei_2, ker_2 en kei_2 are the Kelvin functions of second order [7]. They can be expressed in terms of Kelvin functions of zeroth order and their derivatives. For large *x* (i.e. $t << r$) the Kelvin functions can be approximated by the first term of their asymptotic expansion [7] :

$$ber\,x \approx \frac{1}{\sqrt{2\pi x}}\cos\left(\frac{x}{\sqrt{2}} - \frac{\pi}{8}\right)e^{x/\sqrt{2}} \quad (9)$$

$$ker\,x \approx \sqrt{\frac{\pi}{2x}}\cos\left(\frac{x}{\sqrt{2}} + \frac{\pi}{8}\right)e^{-x/\sqrt{2}} \quad (10)$$

The constants A_i and B_i are to be determined from the boundary conditions. Important is the exponential term because it causes a quick damping of influences at the edges. A rough estimation of the reduction of the forces and moments is obtained by taking the ratio of the positive exponential terms at both edges:

$$\boxed{reduction\ factor :: e^{(x_2-x_1)/\sqrt{2}} = e^{K}} \quad (11)$$

with $$K = \sqrt{\frac{4\sqrt{3(1-\nu^2)}}{t}\,\frac{\tan\gamma}{\cos\gamma}}\cdot(\sqrt{r_2}-\sqrt{r_1}) \quad (12)$$

The V-corrugation is realised by connecting two conical shells of the same top angle but reversely orientated. The 8 constants A_i and B_i can be solved using the four boundary conditions at the edges and the four equations of equilibrium and continuity at the interface.